Saturation of Shear-Induced Isothermal Crystallization of Polymers at the Steady State and the Entanglement–Disentanglement Transition

ARTICLE *in* MACROMOLECULES · OCTOBER 2006

Impact Factor: 5.8 · DOI: 10.1021/ma061143u

3 AUTHORS, INCLUDING:

Weidong Zhang

Technical Center, China State Construction E…

32 PUBLICATIONS **167** CITATIONS

SEE PROFILE

Saturation of Shear-Induced Isothermal Crystallization of Polymers at the Steady State and the Entanglement−Disentanglement Transition

José A. Martins,*,†,‡ Weidong Zhang,†,‡ and António M. Brito†

Departamento de Engenharia de Polímeros, Instituto de Polímeros e Compósitos, Universidade do Minho, Campus de Azurém, 4800-058 Guimarães, Portugal, and CICECO, Universidade de Aveiro, 3810-193 Aveiro, Portugal

Received May 22, 2006; Revised Manuscript Received September 4, 2006

ABSTRACT: To provide insight into the formation of shear-induced precursor structures, three apparently unrelated subjects are analyzed and discussed: the saturation of crystallization from sheared polymer melts, evaluated with a new shear DTA instrument, the steady state in steady shear, and the entanglement−disentanglement transition. It is shown that the same large strains that saturate crystallization also lead to a reversible steady state in steady shear, where the viscosity of the sheared melt is constant in time, and their magnitude is only determined by the temperature of the sheared melt. Features of the melt morphology at this state are discussed, and their importance is highlighted to understand the possible mechanisms behind the formation of shear-induced precursors. Measurements of the reptation time for unsheared samples, and samples sheared up to the steady state, allowed the quantification of the entanglements loss during the transition between these two states (around 2/3), which is interpreted as an entanglement−disentanglement transition. The relevance of this result on assumptions of flow models, particularly the constant number of topological constraints, convective constraint release process, and chain stretch, is discussed.

Introduction

Recent works discussed the crystallization of polymers from stressed melts[1] and the formation of flow-induced shish-kebab precursor structures in entangled polymer melts.[2] A common feature is a discussion of the role played by flow-induced precursors in shear-induced crystallization, particularly their structure and mechanism of formation. From both works, it is clear that details of molecular parameters governing the flow-induced crystallization are unknown, being the discussion focused on possible molecular mechanisms for shish formation and whether there is, or not, a coil−stretch transition in shear flows.

To understand the molecular mechanisms involved in the formation of precursors, the knowledge of the melt morphology in steady shear flows is required. This morphology should be similar for amorphous and semicrystalline polymers melts. Additionally, it is needed information on the stages preceding polymer crystallization. Recent results of large-scale computer simulations on early ordering stages in quiescent polymer melts, before crystallization, provided answers to the last point.[3] It was shown that ordered domains, with high chain mobility, distributed randomly in the melt, coexist with amorphous regions. Dense regions, similar to smectic liquid crystals, grow in the ordered domains. Additional information on early crystallization stages was provided by small-angle oscillatory shear experiments performed on inverse quenched samples.[4] It was detected an additional slow relaxation process at the early crystallization stages (characteristic time ≈1000 s and crystallinity ≈1%), which precedes the liquid-to-solid transition that takes place at low degrees of crystallinity, and shows characteristics of a critical gel behavior. These results allow us to visualize the gradual transition of randomly oriented domains, existing in the supercooled quiescent melt, into the primary nuclei.

When crystallization occurs after shear, it is found an acceleration of the process due to the formation of precursor structures.[1,2] Most of the information on these structures resulted from experiments performed according to a "short-term shearing" protocol in which the effects of intense shear pulses applied at high crystallization temperatures on the crystallization kinetics and morphology development are analyzed.[5] Additional information was provided by real-time SAXS and WAXS experiments performed on specially designed setups.[1,2] The results obtained allowed the construction of a phenomelogical model that explains the enhancement of crystallization from sheared melts.[5] According to this model, shear leads to the formation of "lines" of pointlike nuclei in the flow direction, from which further radial growth takes place. The lifetime of shear-induced precursors, in melts sheared above the melting temperature, was evaluated experimentally by morphological analysis of samples crystallized isothermally, in quiescent conditions, which were preceded by deformations of the melt, by the fiber pull-out technique, and allowed to relax during different times intervals, prior to crystallization.[6] The observation of the anisotropic structures, with cylindritic morphology, or a higher nucleation density around the pulled fiber region, was used to quantify the lifetime of the precursors. It was found that the lifetime is small for high melt temperatures and that it increases by 10^3 for a decrease of 10 deg in the melt temperature. Despite these results, and others mentioned in the literature,[2] two important features that may explain the formation of the precursor structures are unknown so far. One is the nature of the interactions between adjacent chain segments of oriented domains in the molten state. Another is the variation of their size with temperature and deformation in sheared melts.

Knowledge of the morphology in steady shear flows, namely chain conformations and dynamics, was obtained from studies with DNA solutions of different concentration.[7] These results

† Universidade do Minho.
‡ Universidade de Aveiro.
* Corresponding author: e-mail jamartins@dep.uminho.pt; Ph 351 253510325; Fax 351 253510229.

10.1021/ma061143u CCC: $33.50
Published on Web 10/04/2006

are mentioned in this work because there is evidence that features of linear and nonlinear rheology for concentrated polymer solutions and melts are the same.[8] More specifically, it was observed reptation on solutions with a concentration $\sim 13C^*$, where C^* is the overlap concentration. Studies of steady shear flow in dilute and semidilute DNA solutions have shown that, contrary to a prediction of de Gennes,[9] where a coiled state was predicted to exist in shear flow when the rotational component (ω) dominates, a stretched state when the flow is dominated by the elongational component ($\dot{\epsilon}$), and a sharp transition region when $\omega/\dot{\epsilon} = 1$, a fully stretched chain does not exist under shear.[10] Experimental results indicate that the limiting state is the one existing at the transition region, of width $\Delta\omega/\dot{\epsilon} \sim N^{-1}$, where N is the number of Kuhn monomers in one chain. This region may be characterized by a dynamic equilibrium where individual polymer chains continually undergo tumbling motion with large fluctuations in polymer extension. The maximum observed extension in a steady shear flow was around 50% of the full chain length.[7,10,11]

Indirect additional information on the melt morphology at the steady state may be obtained from shear-induced crystallization studies. Previous works indicated that shearing above a critical stress, for a time longer than a critical duration, leads to a saturation of crystallization (limiting crystallization kinetics), being the stress and strain both considered as controlling factors for this saturation.[12] Small-angle light scattering experiments performed with a Linkam shearing cell, using Ziegler−Natta and metallocene polyethylenes (PE), have shown a saturation of the radius $R(\dot{\gamma})$, with a value around 1/2 the radius of the spherulite without shear, at strains of $\sim 10^3$ strain units (s.u.) for the former, while for the latter no saturation was recorded.[13] These large strains also saturate the crystallization of a low-density PE from a sheared melt.[14] The melt state responsible for this saturation was identified as the steady state. Because of the branching of the polymer used in these latter studies, additional characteristics of the steady state were not discussed.

Here we analyze the saturation of crystallization in linear polymers or, more specifically, the effect of melt memory on shear-induced crystallization kinetics. Thus, contrary to the short term shearing protocol,[5,12] the shear pulse was always applied at a temperature higher than the thermodynamic melting temperature. This procedure guarantees that any recorded acceleration of the crystallization kinetics, in comparison with the quiescent process, results only from the sheared melt orientation. However, it must be stressed that other important effects, such as the additional melt orientation imposed during the cooling process or at a specific crystallization temperature, are not considered in this work, although they could be quantitatively evaluated with the shear DTA instrument. Our purpose is to quantify the different contributions to the excess of free energy in sheared melts, although here we restrict this evaluation to the effect of the memory of shear. The melt state responsible for the saturation of crystallization from sheared melts in linear polymers is identified and further analyzed with rheological experiments. The importance of its full characterization is stressed for understanding the structure and mechanisms behind the formation of shear-induced precursor structures. To provide additional information on the melt state where these structures should reach their maximum size and orientation, features of semicrystalline and amorphous polymer melts, sheared up to the steady state, are compared and discussed.

Experimental Section

Shear-induced crystallization studies and rheological experiments were performed with a shear DTA instrument and a rheometer in parallel and cone-and-plate configurations. The material selected was an isotactic polypropylene, Moplen HP501M from Basell, Switzerland, melt flow index of 7.5 g/10 min at 230 °C/2.16 kg, a melting temperature $T_m = 165$ °C, and a thermodynamic melting temperature $T_m^0 = 211$ °C.

In the shear DTA,[15] the molten polymer was initially pumped from the accumulator to the capillary channel at shear rates lower than 0.5 s^{-1}, until the channel was full with molten material, after which a relaxation time of 5 min was allowed for melt relaxation. Shear pulses, of different duration and intensity, were then applied, after which the material was cooled to the crystallization temperature, with a constant and controlled cooling rate, and the crystallization kinetics was recorded. The apparent shear rate at the wall was corrected with the Rabinowitsch correction for the non-Newtonian behavior of the material. The true shear rates were used to evaluate the strains of the melt.

A Physica MCR 300 rheometer (Paar Physica), with parallel plate (25 mm diameter) and cone-and-plate (25 mm plate diameter and 2° cone angle) configurations, was used to perform the shear stress-growth, oscillatory, and steady-shear experiments. The average true sample temperature was evaluated from the nominal temperature of the experiments following a temperature calibration procedure described previously.[16] This temperature was recorded with an accuracy of ±1 °C, and the gap size was 0.7 mm for all experiments. For each rheometeric experiment a new sample was used, and the experimental conditions were controlled to ensure data reliability. Also with this purpose, some experiments were repeated in a Rheologica Stresss Tech (Rheologica Instruments AB, Sweden).

Effect of Melt Memory on Crystallization Kinetics

The results of Figure 1, obtained with the shear DTA instrument,[15] show the isothermal crystallization of iPP at 125 °C, after controlled shearing at 220 °C, at constant shearing time and different shear rates (Figure 1a) and at constant shear rate and different shearing times (Figure 1b). The crystallization kinetics is accelerated by the increase of the shear rate or of the shearing time, and saturation occurs for a constant applied strain (1962 s.u. on average).

At higher melt temperatures, saturation of crystallization at the same temperature is delayed (Figure 1c), and it occurs at lower strains. This behavior is consistent with previous results,[1,12] where it was found that long-lived structures, generated during shear, appear at shorter times (lower strains) at higher temperature, but the temperature dependence of the critical strain was not evaluated. The increase of the half-crystallization time with the sheared melt temperature (Figure 1c) suggests that the long-lived structures generated at high temperatures have smaller size. A similar temperature variation was found for the smectic periodicity in sheared iPP melts.[17]

Starting from the same sheared melt temperature, the crystallization at different temperatures saturates at the same strain (Figure 1d). We refer to this strain as critical strain. The critical strain is thus independent of the crystallization temperature. It depends only on the temperature of the sheared melt. Besides confirming strain as the controlling factor for saturating the shear-induced crystallization, these results also indicate that a well-defined melt state must be responsible for this saturation.

Identification of the Melt State Responsible for the Saturation of Crystallization

The existence of a steady state with constant entanglement density may be confirmed by shear stress-growth experiments, which are well documented in the literature, since they may be performed with solutions of different concentration and melts of amorphous or semicrystalline polymers. The variation of viscosity (or shear stress) with time, at constant shear rate, stabilizes at a constant value, the steady state, where the density

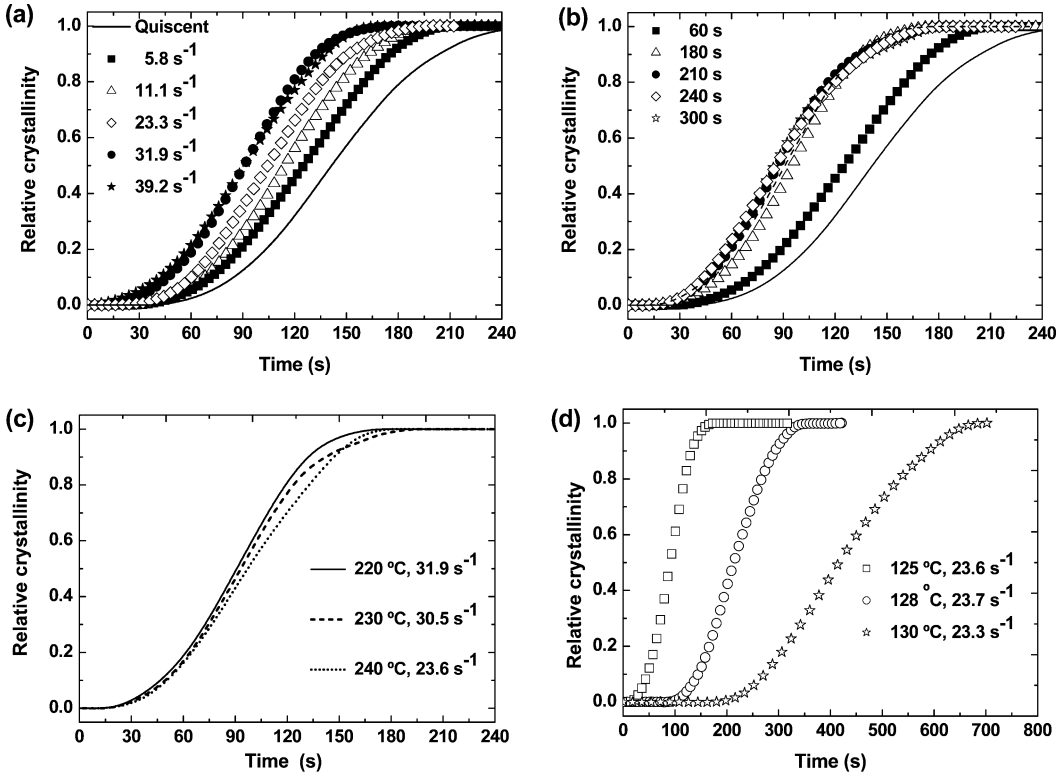

Figure 1. Isothermal crystallization of iPP recorded with the shear DTA. Nominally isothermal crystallization at 125 °C after shearing the melt at 220 °C with (a) constant shearing time (60 s) and increasing shear rates—saturation at $\dot{\gamma}_w = 31.9\ s^{-1}$ corresponding to a $\gamma_w = 1914$ s.u—and (b) constant shear rate of $\dot{\gamma}_w = 9.6\ s^{-1}$ and increasing shearing time—saturation at $\gamma_w = 2016$ s.u. Solid lines are for quiescent crystallization. (c) Saturation of crystallization at 125 °C for different shearing melt temperatures. The shearing time is 60 s, and the average critical strains are 1914, 1830, and 1416 s.u. for 220, 230, and 240 °C, respectively. (d) Saturation of crystallization at different crystallization temperatures and the melt temperature of 240 °C for constant shearing time of 60 s and the shear rates indicated. The average critical strain is 1412 s.u. The measurement error in the strain values is ±10%.

of entanglements in the sheared melt is constant. We define the time when the polymer melt reaches the steady state, evaluated following the procedure of Figure 2, as the onset of the steady state. For example, for polybutadiene solutions, the onset of the steady state appears at a constant strain, around 11 s.u. (Figure 8 of ref 18). Earlier experiments, performed with low-density polyethylene melt at 150 °C, indicated a strain at the onset of the steady state of around 2000 s.u. (Figure 2 of ref 19, for the shear rates of 10 and 20 s^{-1}).[19] Since these experiments are performed at a constant shear rate, further on we refer to this state as the steady state in steady shear.

Although the existence of this steady state was extensively recognized, attention has been mainly focused to the fitting quality of theoretical models to the experimental data at the transition from a viscoelastic linear regime to the viscoelastic nonlinear regime. Only recently, the flow of a 1,4-polybutadiene solution in a cone-and-plate shear cell was visualized using the particle tracking velocimetry technique at the start of the flow, at the overshoot and during the undershoot, and at the steady state.[20] These results allowed concluding for the nonlinearity of the velocity profile during a simple shear flow at the steady state, which is consistent with a previously reported entanglement−disentanglement transition.[21]

Analysis of other relevant and interesting features, such as the evaluation of the strain at the onset of the steady state, mentioned above for some published results,[18,19] and its variation with the sheared melt temperature was, to our knowledge, never performed. We report here the evaluation of the strain at the onset of the steady state for iPP at 220 °C with the parallel plate (Figure 2a) and cone-and-plate configurations (Figure 2b). The latter results are around 2/3 the values measured with the parallel plate configuration. For the same melt temperature, the magnitude of the strain at the onset of the steady state evaluated with the latter configuration is similar to that obtained with the shear DTA (see Figure 4a and the discussion below). From now on, we call the strain at the onset of the steady state the critical strain. The effect on the critical strain of the initial residence time (without shearing) at the shearing temperature was also evaluated. Figure 2b shows these results for the cone-and-plate configuration. The data for 5 s^{-1} are indicative of the difference in the results obtained, regardless if the experiments were performed with different, or similar, residence time at the melt temperature. The measurement error of the critical strain values is around 10%.

Clearly, the same strain that saturates crystallization is also required for the establishment of a steady state in steady shear. A critical strain may then be defined as the minimum value of strain to align, with a limiting orientation angle,[22] at a specific temperature, the maximum number of chain segments with the flow direction.

Additional Characterization of the Steady State for Linear Polymers

The excellent agreement between the critical strain values measured with different instruments suggests that the knowledge of the melt morphology at this state is of utmost importance to explain the formation of shear-induced precursors. However, because of the large time needed at low shear rates to reach this state, the validity of any information there obtained may be questioned. To ensure its validity, it was verified the reversibility of the steady state, the time−shear rate superposition of the transient viscosity measured at different, constant,

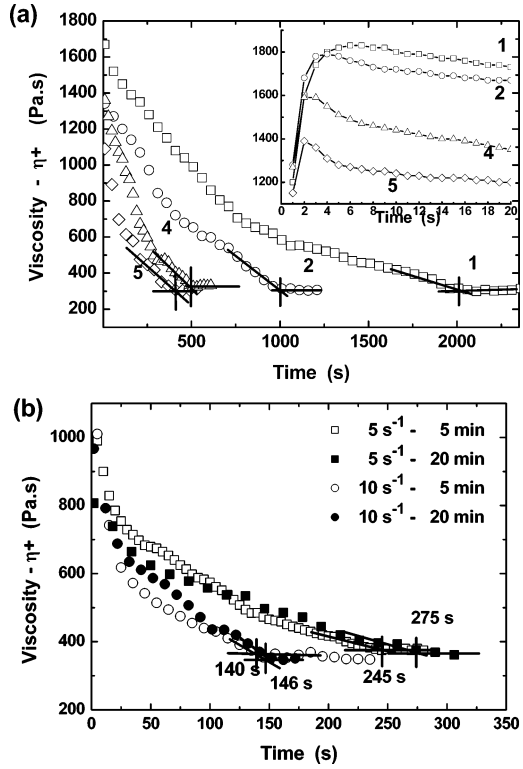

Figure 2. Results of stress growth in shear for isotactic polypropylene. Transient viscosity measured at 220 °C with the parallel plate (a) and cone-and-plate (b) configurations at the shear rates indicated. The solid lines show the evaluation of the critical strain (indicated by the vertical lines) at the onset of the steady state. The inset in (a) shows the behavior recorded for short shearing times. The average critical strain is ≈1970 s.u. for the parallel plate results and ≈1360 s.u. for the cone-and-plate results. The measurement error in the strain values is ±10%.

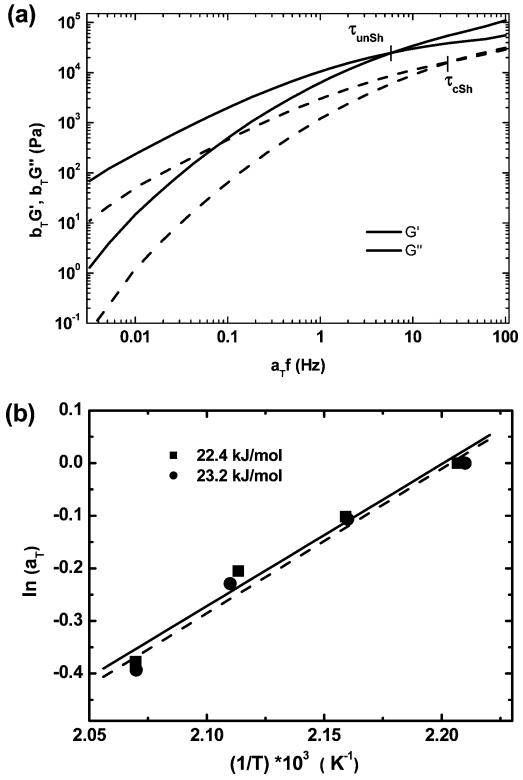

Figure 3. Oscillatory shear results for isotactic polypropylene. (a) Reduced curves of unsheared (solid lines) and critically sheared (dashed lines) samples at the reference temperature of 177 °C, evaluated considering the temperature-dependent frequency and modulus shift factors, a_T and b_T, respectively. The reptation time was evaluated at the intersect frequency between G' and G''. (b) Activation energy evaluated from oscillatory shear experiments of unsheared (squares) and critically sheared (circles) samples.

shear rates, and the similar cooling scans obtained for critically sheared and unsheared samples. Results of these experiments, described in the Supporting Information, guarantee that the oscillatory shear analysis of this state, whose results are presented below, is not masked by other side effects.

For this characterization it was ensured that for both the unsheared and the critically sheared samples (sheared up to the onset of the steady state), at all temperatures and in the oscillation frequency range tested, the flow behavior is viscoelastic linear. Although the transition to the steady state, in steady shear, is viscoelastic nonlinear, this melt state may be probed by experiments in the viscoelastic linear regime. The same constant stress (400 Pa) was used to analyze the differences in the reptation time of unsheared and critically sheared samples. For these last samples, the same shear rate (5 s^{-1}) was used for establishing the steady state at the different temperatures, after which the oscillatory shear experiments were performed.

Figure 3a shows the reduced curve of G' and G'' at 177 °C for unsheared and critically sheared samples, which have lower reptation time. We assumed that the crossing point frequency between $G'(\omega)$ and $G''(\omega)$ corresponds to the inverse of the reptation time.[23] The oscillatory shear flow activation energy may be considered to be the same for both melt states, ≈22.5 ± 0.7 kJ/mol (Figure 3b). The obvious conclusion is that the barriers to flow in this regime, in both melt states, are the same. They result only from the conformational energy barriers and the rigidity of the network, which increases when the polymer is slightly cross-linked or when stronger interactions exist at the molten state. Systematically slightly larger values were obtained for the oscillatory shear flow activation energy of critically sheared samples, which we assumed to result from the effect of the larger precursor structures on the flow resistance.

The critical strain, either the one measured at the onset of the steady state or that needed to saturate the crystallization from a sheared melt, measured with the shear DTA instrument, (Figure 4a), showed a similar temperature dependence, and both approach a limiting value at high temperatures. For the reptation time, a similar behavior was observed (Figure 4b). These results suggest that the degree of orientation reached by the chain segments, and therefore the orientation of the precursor structures with the flow direction, at the steady state have reached a limiting lower value. On the other hand, the precursor structures must have reached, at this state, their largest size. We will discuss further on this point.

A surprising result is obtained when the reptation times of unsheared and critically sheared samples are compared (Figure 4b), the latter being around 1/3 the time of the former. Identical results were also obtained for branched polyethylene melts,[14] but specifically for sheared polyethylene melts, a different relationship was obtained between the reptation time measured at the two states. So far, we cannot fully explain this result, but we suspect that it results from the symmetry of the polymer chain along the backbone.

Sheared melts of amorphous polymers have exactly the same behavior as that recorded for iPP. Because of the larger critical strains at the onset of the steady state, a commercial grade of polystyrene ($M_w = 2.71 \times 10^5$ g/mol, $M_w/M_n = 2.0$, MFI = 2 g/10 min, Innova S.A., Brazil) was selected to illustrate the behavior of amorphous polymers (Figure 5). The temperature variation of these strains is similar to those of semicrystalline

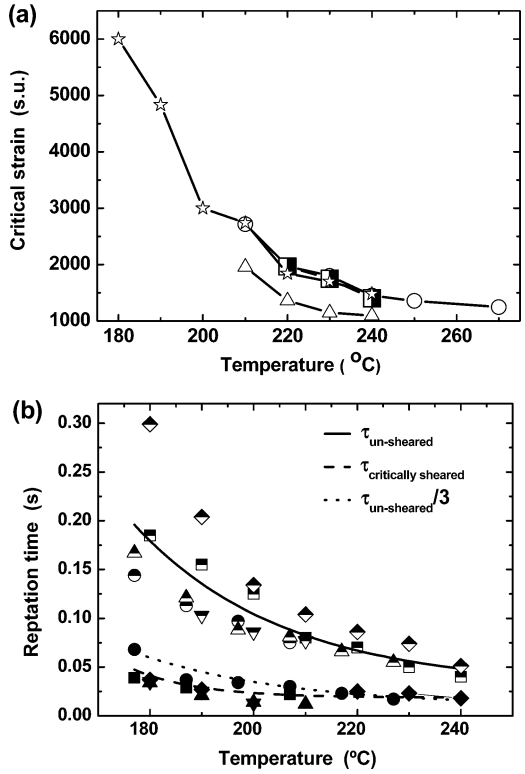

Figure 4. Temperature variation of the critical strain and reptation time for isotactic polypropylene. (a) The critical strain measured with the shear DTA (half-filled squares), at the onset of the steady-sate in shear stress growth experiments in cone-and-plate (triangles) and parallel plate (circles and stars for experiments performed with a Paar Physica and Rheologica Stress Tech rheometer, respectively) configurations are plotted as a function of the sheared melt temperature. (b) Reptation time measured at different temperatures for unsheared (half-filled symbols) and critically sheared (full symbols) samples. These results were obtained from sets of experiments performed with the two rheometers indicated above. The solid and dashed lines are fits of a single-exponential decay function to the average values. The dotted line is the division by three of the reptation time for the unsheared samples. The dispersion in the data increases clearly for temperatures lower than the thermodynamic melting temperature of the polymer (211 °C).

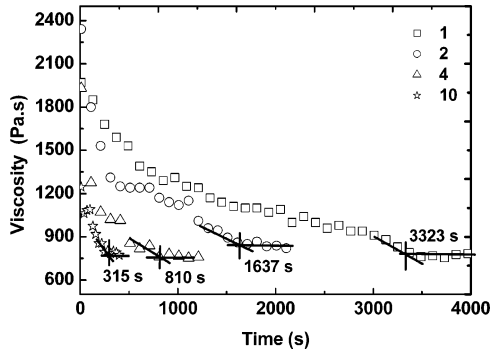

Figure 5. Shear stress growth results for polystyrene. Transient viscosity measured at 220 °C with the parallel plate configuration for polystyrene. The shear rates and the time at the onset of the steady state are indicated. The average critical strain is 3247 s.u. (±10%).

polymers (Figure 6a). Also, the reptation time at the steady state is 1/3 lower than that of unsheared samples (Figure 6b).

From the above results, and others presented in the literature, the steady state in steady shear may be characterized by (1) large critical strains at its onset, which decrease with the melt temperature; (2) for semicrystalline polymers these strains saturate the crystallization[13,14] and the anisotropy of sheared iPP melts evaluated by SAXS patterns, at strains of around ~10^3 s.u.;[24] (3) the critical strains must also be linked to the size and orientation of the shear-induced precursor structures; (4) to explain the lower critical strains at higher temperatures, the precursor structures must have lower size,[14] which is an assumption consistent with experimental results;[17] and (5) melts of amorphous polymers at the steady state must also have oriented structures, which are not precursor structures because crystallization is inhibited in atactic polymers, but they should explain the orientation, on a molecular basis, shown by highly strained melts.

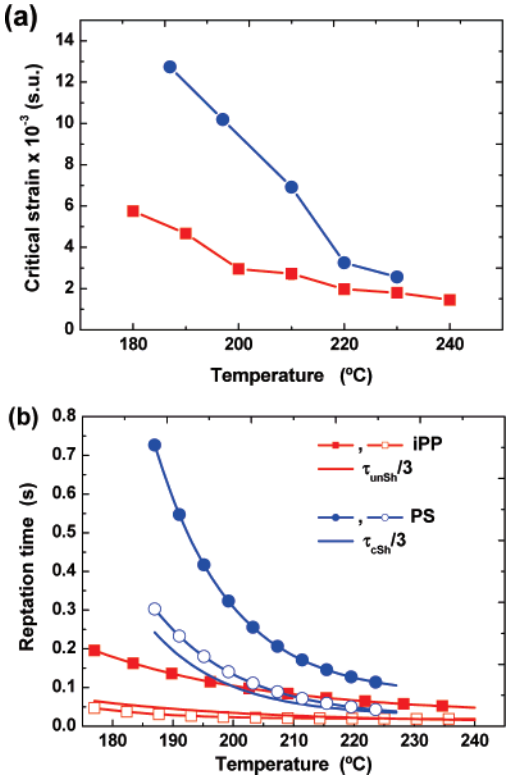

Figure 6. Comparison between the temperature variation of the critical strain and reptation time for amorphous and semicrystalline polymer melts. (a) Temperature variation of the critical strain at the onset of the steady state for isotactic polypropylene (squares) and polystyrene (circles). (b) Temperature variation of the reptation time for the same materials for unsheared (filled symbols) and critically sheared samples (open symbols).

Melt Morphology at the Steady State and Shear-Induced Precursor Structures

Some characteristics of the steady state, all based on experimental results, were identified. However, a full picture of the melt morphology at this state is not yet available, and it is crucial for understanding the molecular origin of shear-induced precursor structures. Since the melt state that saturates the crystallization also appears in melts of amorphous polymers and in polymer solutions, studies of these materials at the steady state may provide us with important information for understanding the physical origin of shear-induced precursors.

One common result, mentioned previously, is the lower reptation time of critically sheared samples (Figures 4b and 6b). It indicates that the number of constraints of a sheared melt at the steady state is smaller. This is explained by an entanglement−disentanglement transition,[21] which was reported to occur in controlled-stress experiments of polymer solutions, for stresses higher than a critical value, determined by the crossover modulus G_c, given by $G'(\omega_c) = G''(\omega_c)$. Upon the transition the sample reaches a steady state. For the highest applied

stresses, a difference in viscosity of $\sim 10^3$ Pa·s between the initial and the steady states was measured. It was ascribed to a massive loss of entanglements (entanglement−disentanglement transition), which was found to show no hysteresis (see also Appendix).

Although this transition was observed for polymer solutions, it must also occur in polymer melts since the same state, the steady state, is the final state of the transition for both polymer solutions and melts. However, this state is not disentangled. Therefore, the entanglement−disentanglement transition would be better classified as a transition to the steady state. Because of experimental limitations, the initial number of entanglements, which may be evaluated from the plateau modulus value, was not evaluated in the present work. However, the reduction of entanglements may be estimated by comparing the reptation time for unsheared and critically sheared samples. The ratio between the reptation time at the two states, unsheared (u) and critically sheared (c), is equal to the ratio between the number of entanglements (Z) in each state, $\tau_u/\tau_c = Z_u/Z_c$. The results obtained for iPP and PS, among others materials analyzed, indicate that only $\sim$1/3 of the initial entanglements remain at the steady state. The initial number of entanglements is recovered for iPP and PS when the sample is cooled below the melting or the glass transition temperature, respectively (see Supporting Information).[25]

The melt morphology at the steady state may further be characterized by conformational states parallel and perpendicular to the flow direction, the latter decreasing with the shear rate increase,[26] and a smaller number of entanglements. The relatively lower viscosity at higher shear rates should result from a stronger alignment with the flow direction of some conformational states. Therefore, the oriented precursor structures in sheared melts of semicrystalline polymers should reach their maximum size and orientation with the flow direction at the steady state, where they coexist with a dynamic melt,[27] in which the polymer chains continuously undergo extensions and tumbling motion, without ever reaching a full extension, thus precluding the existence of a fully stretched state in steady shear.[10,11] The same behavior is expected for critically sheared melts of amorphous polymers. They also should reach their maximum anisotropy at the steady state, which should decrease with the temperature of the sheared melt.

Apparently, the obvious conclusion from our data is that "shearing produces an equilibrium state of entanglement, and that the concomitant orientation and stretching of the partially disentangled chains in the network are what contribute to the nucleation enhancement".[28] This comment is quoted here because it helps us to better illustrate the meaning of the above discussion, the discussions below, and to get an idea of the implications that the explanation for the molecular origin of shear-induced precursor structures may have.

Of course, the steady state may be considered an equilibrium state of entanglements. But it cannot be the stretching of the partially disentangled chains in the network, between the surviving entanglements, at the steady state, what contribute to the crystallization enhancement. There are two reasons, based on experimental results that support the above statement. First, the reptation time at the steady state is small. Thus, during the cooling process, from the melt to the crystallization temperature, the extended chains between entanglements must relax very fast to higher entropic states. (It must be noted that this work is focused on the effect of the melt memory on shear-induced crystallization and that strains are applied at temperatures above the thermodynamic melting temperature.) The second reason results from the effect that the finite size of ordered regions between entanglements may have on the flow activation energy. The results of Figure 3b clearly show that unsheared and critically sheared melts, which have 1/3 of the initial entanglements, have the same flow activation energy in the viscoelastic linear regime. Since the appearance of ordered regions between entanglements must necessarily imply the existence of physical interactions between segments of adjacent chains, one would expect that the formation of these ordered regions between entanglements would lead to higher activation energies for critically sheared melts.

Knowing the size of precursor structures, this increase could be estimated. Information on their dimensions is scarce. Furthermore, it was proved that their size is temperature dependent,[17] and it must also be strain dependent.[24] Besides the anisotropic structures of $\sim$500 Å in the flow direction mentioned previously,[24] also for iPP, SAXS experiments allowed the identification of layers containing long-lived polymer molecules, separated by unoriented chains.[29] The average spacing between layers was $\approx$430 Å. The periodicity evaluated for the shear-induced smectic phase was $\approx$40 Å.[17]

The interacting potential W of two parallel chain molecules separated by a distance r, with length L, each molecule in one chain having a molecular diameter of σ, is[30]

$$W = -\frac{3\pi CL}{8\sigma^2 r^5} \tag{1}$$

where C is related to the number density of molecules in each chain (ρ) by the Hamaker constant $A = \pi^2 C\rho^2$. It was assumed the same density of molecules for each chain. Details about the evaluation of the Hamaker constant for polypropylene may be found in the Supporting Information. This constant may be calculated from the Lifshitz theory of the van der Waals interactions, where the interacting forces are derived in terms of dielectric constants and refractive indexes. The value obtained for two polypropylene chains interacting across vacuum is $A = 7.1 \times 10^{-20}$ J. The distance r between the two chain outer surfaces is assumed to be the same as the molecular diameter. With $\sigma = r = 5.57$ Å and $C = 6.6 \times 10^{-78}$ J m^6, the interaction potential as a function of L (in angstroms) is $\approx -28.2L$ J/mol. Thus, two parallel iPP chains, between entanglements, with a length of 100 Å, yield an interaction potential of -2.82 kJ/mol, which should result in an identical increase on the oscillatory shear flow activation energy. The value considered for the length of shear-induced precursors (100 Å) is a typical thickness of a lamella. Results of our work, not yet published allowed to estimate the size of shear-induced precursor structures from the free energy excess of critically sheared iPP melts. The values obtained were between 300 and 500 Å for the length and between 30 and 60 Å for their thickness.

These results, those of Figure 5 obtained for sheared polystyrene melts, and the characteristics of the steady state described above, based on literature results[10,11,13,17,24,26,27] and on our own work,[14] led us to question the physical nature of entanglements. Shear-induced precursor structures seem to be intimately related with entanglements. Since the above results indicate that they cannot be created between entanglements, it remains that entanglements, themselves, should be at the origin of those structures. This is the reason for our discussion on shear-induced precursors, the melt morphology at the steady state, and entanglements. This specific subject will be discussed further on in future works.

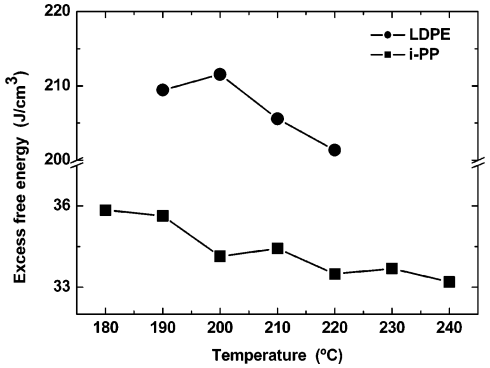

Figure 7. Temperature variation of the excess free energy at the onset of the steady state.

Evaluation of the Excess Free Energy in the Critically Sheared Melt

It is commonly accepted that crystallization from strained melts results from thermally-induced and flow-induced processes, each one giving its own contribution to the overall free energy of the melt. These two effects were recently included into a two-phase simulation model of the melt spinning for poly(lactic acid).[31] The model included a nonisothermal version of the Avrami equation, which was coupled with a nondimensional free energy of the amorphous phase that accounts for the effect of flow. One model prediction is that flow-induced crystallization occurs only in a temperature range where quiescent, thermally-induced, crystallization occurs. This result stresses the importance of evaluating the excess of free energy in a strained melt, which results from both the deformation of the melt at temperatures higher than the melting temperature of the polymer and further deformations, under real processing conditions, of the supercooled melt. The analysis of the last effect, following the short-term shearing protocol mentioned previously,[5,12] allowed to conclude that the density of nuclei in sheared supercooled melts increases with the applied specific work up to a limiting value of around 10^{18} nuclei/m^3.[32,33]

Evaluation of the excess of free energy resulting from melt memory effect on flow-induced crystallization is presented below. The purpose of this exercise is to show that the results presented in this work are consistent with predictions of an evaluation for the free energy increase in a sheared melt resulting from the orientation imposed by the flow.[34] This evaluation assumes the absence of chain stretch. The excess of free energy per unit volume (A) was evaluated from the orientation tensor $\mathbf{S}$, considering the volume-preserving condition ($\lambda_1\lambda_2\lambda_3 = 1$) and that the anisotropy resulted from a single step deformation of eigenvalues λ_1, λ_2, λ_3. Following the nomenclature and definitions of ref 31, the expression obtained for the excess of free energy with respect to the undeformed state was $A = G \ln[(\lambda_1 + \lambda_2 + \lambda_3)/3]$, with $G = 6G_N^0 = 6\rho RT/M_e$. A different expression for the excess of free energy, derived from the Doi−Edwards independent alignment approximation model,[35] is $A/G \propto De^2$, where De is the Deborah number, the proportionality constant being dependent on the nature of the flow filed, shear or elongational.

The excess of free energy per unit of volume evaluated at different melt temperatures for the iPP used in this work and LDPE[14] is plotted in Figure 7. Only the critical strains at different sheared melt temperatures measured with the shear DTA were used in this evaluation. The other parameters, namely M_e and ρ, were obtained from ref 35. Considering a unidirectional flow, the strain at the onset of the steady state that saturates crystallization is approximately equal to λ_1, and the incompressibility condition may be used to evaluate λ_2 and λ_3. Taking into account the assumptions of the model and the one made here, related with the directionality of the flow, the results obtained are approximations that are nevertheless important to support both our explanations and the physics behind the derivation of the excess free energy.

The higher value obtained for LDPE results mainly from the lower molecular weight between entanglements of this polymer. The free energy decreases with the melt temperature, indicating that the orientation state of the melt at higher temperatures is lower, which is consistent with our previous assumption that the size of precursor structures decreases with the temperature of the sheared melt. Conversely, at lower melt temperatures, the larger size of precursor structures explains the larger strains needed to saturate the crystallization (Figure 1c) and establishing the steady state in steady shear and also the higher values obtained for the excess of free energy.

Since the free energy is only a function of the sheared melt temperature and the molecular orientation at the steady state, which depends on a critical strain, it has a limiting value at this state. It is this limiting high value that also explains the reason why crystallization at different temperatures, starting from the same sheared melt temperature, saturates at the same strain (Figure 1d), the one needed to establish the steady state in steady shear.

Implications on Assumptions of Tube Models and on the Nature of Convective Constraint Release Process

Theories used for the description of the flow of polymer melts under the action of strong deformations usually consider the flow of a test chain in a tube whose diameter is determined by constraints formed by the surrounding chains. The relaxation mechanisms considered are reptation, thermal and convective constraint release, and chain stretch, among others, such as double reptation and tube dilatation, all of them contributing for a decrease of the reptation time evaluated from the Doi−Edwards original theory.[36] The number of constraints imposed by the surrounding chains to the test chain is generally considered constant. For the chain stretch it is also considered an increase in the number of constraints with the primitive path length of the test chain.[37] Since the results obtained in this work indicate that the number of entanglements at the steady state is 1/3 of their initial number, clearly some of the above-mentioned assumptions must be questioned.

By the same reason, another point that is questioned is the physical interpretation for the microscopic origin of the convective constraint release process (CCR). The CCR and chain stretch processes were introduced to explain the nonlinear viscoelastic properties of entangled polymers under large strains and/or fast flows.[36−39] Originally, the activation of CCR process was envisaged in the following way: once a chain is stretched by a large step strain, it retracts along the tube abandoning some entanglement points. The CCR mechanism activates then the surrounding chains that were initially constrained by the test chain, contributing therefore, besides reptation, as an additional process for the renewal of the entanglement topology.[38,39] A different microscopic theory of nonlinear melt flow considers a local CCR process.[40] It is considered that local CCR generates local Rouse jumps of the tube, reorienting the chain segments both toward and away from the flow direction. Most importantly, it is further assumed that neither the tube segments per chain (number of entanglements per chain) nor the tube diameter changes.[37,40] The practical effect of these approaches was discussed with detail in the literature,[36,37] and current challenges

regarding the way of operation of CCR process were also analyzed.[41] It produces a state of the melt almost invariant with changes of flow rate, yielding a saturation of the chain anisotropy.

We will focus here in comparing model predictions with experimental results of the start-up of shear, such as those of Figure 2a. In these experiments it is known that the stress overshoot at lower strains results from the large driving force to stretch the tube, which is induced by the onset of the flow (see inset in Figure 2a). This force decreases when the chains become oriented with the flow direction. The incorporation of CCR and chain stretch into the flow models allows predicting this stress overshoot. It also allows capturing the steady-state values; i.e., the combination of the two processes is required for a description of the transition from the overshoot up to the steady state.

It is interesting now the confrontation of the above different descriptions of CCR process with the experimental results obtained for the visualization of the flow in a cone-and-plate shear cell before the overshoot, during the transition (undershoot) to the steady state, and at this state.[20] After the stress overshoot, it was found that the velocity profile between the cone and plate was nonlinear for non-Newtonian fluids. This nonlinearity was found to be consistent with an entanglement−disentanglement transition (see Appendix).

Since considering the experimental results known so far, it is reasonable to expect that for lower strains (before the stress overshoot) there is not a change in the number of constraints of the tube, and since the final number of entanglements is 1/3 smaller than the initial number, we can reasonably consider that the undershoot in the above-mentioned curves results from a decrease in the number of entanglements.

Now, we must remember that the two coupled processes that allow the description from the overshoot up to the steady state, CCR and chain stretch: one considers a constant number of entanglements and constant tube diameter while the other considers its increase.[37] In some versions of the chain stretch it is also considered a constant number of entanglements. These assumptions are clearly inconsistent with the experimental data presented here.

Conclusions

This work has provided information on the magnitude of strains needed in sheared melts for reaching steady state and their temperature dependence. It was shown that cooling a sheared melt from this state saturates the crystallization. The steady state is reached after a transition in which around 2/3 of the entanglements are destroyed. The steady state is not a disentangled state. Since a fully disentangled state does not exist at the steady state, the previously reported entanglement−disentanglement transition, observed for well entangled polymer solutions,[21] should be more accurately described as a transition to the steady state.

Contrary to conclusions of other recent works, these results demonstrate that forced flow at high temperatures does not lead to a remelting of precursors[42] and that the lifetime of shear-induced precursors, at steady state, is much longer than that previously estimated.[6] Although the molecular mechanism behind the formation of shear-induced precursor structures is not yet established, it is shown that these structures coexist at steady state with a less entangled melt and that their size should decrease with the sheared melt temperature. On the other hand, the orientation of precursor structures in the flow direction should increase with the strain applied to the molten polymer, up to a limiting steady-state value.

Other relevant results of this work are the demonstration that the oscillatory shear flow activation energies are the same for unsheared and critically shearead samples, although the reptation time of the latter is shorter. The surprising similar behavior shown by sheared melts of amorphous polymers concerning the temperature dependency of the strain at the onset of the steady state, the also similar oscillatory shear flow activation energy for unsheared and critically sheared samples, and the lower reptation time shown by the latter samples defy the presentation of a molecular mechanism for the formation of the shear-induced precursor structures. They cannot be created in the extended chains between entanglements since this would increase the oscillatory shear flow activation energy for the critically sheared samples. The identification of a molecular mechanism for their formation implies questioning the physical nature of an entanglement.

The results presented in this work also raise several other questions. Why are $^2/_3$ of the initial entanglements destroyed during the transition up to the steady state, while $^1/_3$ remain? Are there "weak" and "strong" entanglements, the latter surviving up to the steady state? How can we envisage the coexistence of precursor structures with a dynamic melt at the steady state? What are the physical interactions that sustain the precursor structures, and how can they be made consistent with topological constraints? In our opinion, the answer to these questions implies the analysis of what is considered to be a topological constraint. Do topological constraints effectively play the role that is assigned to them? After all, "there are no topological obstacles in a system of linear chains since, given sufficient time, a chain can diffuse and release all topological restrictions".[43]

Acknowledgment. We thank J. J. Cruz Pinto, A. C. Diogo, J. M. Maia, and J. Covas for comments and discussions and Paulo Lopes for a careful reading of the final manuscript and suggestions to clarify some of its contents. We also thank Michael Rubinstein and Henning Winter for reading earlier versions of this work. The two reviewers of this work are also acknowledged for useful comments. This research was supported by the European Community fund FEDER through the project POCTI//CTM/46270/2002 approved by the Portuguese Foundation of Science and Technology (FCT), which is also acknowledged for the grant BPD/5517/2001 assigned to W. Zhang.

Appendix. The Entanglement−Disentanglement Transition

The conditions under which this transition occurs were described above, and they may also be found in the original work.[21] In the following, it will be shown that the state reached after the transition is not a disentangled state and that this transition would be more appropriately described as a transition to the steady state.

The viscosity at the steady state must be a property of the material, and its value should be independent of the device used, or the experimental protocol followed, to reach that state. For high shear rates (500 s^{-1}) the steady state reached at constant shear rate or constant stress is characterized by the same viscosity. The steady shear viscosity is ≈12 Pa·s for the experiments performed at 500 s^{-1} (Figure 2 of ref 21). The constant shear stress of 5 kPa yield a steady state at the shear rate of 500 s^{-1}, with a viscosity of ≈10 Pa·s (Figure 6a of ref 21). Surprisingly, the experiments performed at lower stresses

yield steady states with relatively lower viscosities than those performed at a constant, lower, shear rate. For example, for the shear rate of 40 s^{-1} steady-state viscosities of ≈110 and ≈60 Pa·s are obtained for the constant shear rate and constant stress experiments (Figure 8 of ref 21). The discussion for the source of these different values is outside the scope of this work. They are assigned by the authors to the different flow responses of entangled polymer solutions under constant shear rate or constant stress experiments. This conclusion, however, implies the existence of a window of shear stress (between 2 and 5 kPa for the solution tested)[21] in which the viscosity at the steady state evaluated from constant stress experiments is lower than that evaluated from constant shear rate experiments. From a physical point of view it is difficult to support this conclusion.

Although the entanglement−disentanglement transition was apparently exclusively assigned to constant-stress experiments, the above discussion shows that it is also recorded with constant shear rate experiments, such as the shear stress growth experiments described in this work. Regardless of the test method used, the final "disentangled" state is a steady state, and so, the entanglement−disentanglement transition would be better classified as a transition to the steady state. The proof that the steady state is not a disentangled state and that the entanglement−disentanglement transition is related to the destruction of $^2/_3$ of entanglements on the transition to the steady state is easily made by the finite values of the reptation time measured at the steady state (Figures 4b and 6b).

Supporting Information Available: Additional information on the characterization of the steady state, additional information on the results of Figures 4b and 6b, evaluation of the Hamaker constant for polypropylene, and Figures S1 and S2. This material is available free of charge via the Internet at http://pubs.acs.org.

References and Notes

(1) Kumaraswamy, G. *J. Macromol. Sci., Part C* **2005**, *45*, 375 and references therein.
(2) Somani, R. H.; Yang, L.; Zhu, L.; Hsiao, B. S. *Polymer* **2005**, *46*, 8587 and references therein.
(3) Gee, R. H.; Lacevic, N.; Fied, L. *Nat. Mater.* **2006**, *5*, 39.
(4) Coppola, S.; Acierno, S.; Grizzuti, N.; Vlassopoulos, D. *Macromolecules* **2006**, *39*, 1507.
(5) Liedauer, S.; Eder, G.; Janeschitz-Kriegl, H.; Jerschow, P.; Geymayer, W.; Ingolic, E. *Int. Polym. Process.* **1993**, *8*, 236.
(6) Azzurri, F.; Alfonso, G. C. *Macromolecules* **2005**, *38*, 1723.
(7) Hur, J. S.; Shaqfeh, E. S. G.; Babcock, H. P.; Smith, D. E.; Chu, S. *J. Rheol.* **2001**, *45*, 421.
(8) Paul, K.; Binder, W.; Heermann, D. W.; Kremer, K. *J. Chem. Phys.* **1991**, *95*, 7726.
(9) de Gennes, P. G. *J. Chem. Phys.* **1974**, *60*, 5030.
(10) Smith, D. E.; Babcock, H. P.; Chu, S. *Science* **1999**, *283*, 1724.
(11) Schroeder, C. M.; Teixeira, R. E.; Shaqfeh, E. S. G.; Chu, S. *Macromolecules* **2005**, *38*, 1967.
(12) Kumaraswamy, G.; Issaian, A. M.; Kornfield, J. A. *Macromolecules* **1999**, *32*, 7537.
(13) Chai, C. K.; Auzoux, Q.; Randrianatoandro, H.; Navard, P.; Haudin, J. M. *Polymer* **2003**, *44*, 773.
(14) Zhang, W.; Martins, J. A. *Macromol. Rapid Commun.* **2006**, *27*, 1067.
(15) Martins, J. A.; Zhang, Wd.; Brito, A. M.; Infante, U.; Romero, M.; Soares, F. O. *Rev. Sci. Instrum.* **2005**, *76*, 105105.
(16) Martins, J. A.; Zhang, Wd.; Carvalho, V.; Brito, A. M.; Romero, M.; Soares, F. O. *Polymer* **2003**, *44*, 8071.
(17) Li, L. B.; de Jeu, W. H. *Faraday Discuss.* **2005**, *128*, 299.
(18) Menezes, E. V.; Graessley, W. W. *J. Polym. Sci., Polym. Phys. Ed.* **1982**, *20*, 1817.
(19) Wagner, M. H.; Meissner, J. *Makromol. Chem.* **1980**, *181*, 1533.
(20) Tapadia, P.; Wang, S.-Q. *Phys. Rev. Lett.* **2006**, *96*, 16001.
(21) Tapadia, P.; Wang, S.-Q. *Macromolecules* **2004**, *37*, 9083.
(22) Mhetar, V. R.; Archer, L. A. *J. Polym. Sci., Part B: Polym. Phys.* **2000**, *38*, 222.
(23) The assumption that the crossing point frequency between $G'(\omega)$ and $G''(\omega)$ corresponds to the inverse of the reptation time results directly from the fact that, in the linear viscoelastic regime, $G'(\omega)$ and $G''(\omega)$ are the sine and cosine Fourier transforms of the relaxation modulus. Using the Doi−Edwards theory, $G'(\omega)$ is given by eq 7.45, p 228 of: Doi, M.; Edwards, S. *The Theory of Polymer Dynamics*; Oxford University Press: New York, 1986. A similar expression may be obtained for $G''(\omega)$, the only difference being the numerator of the right-hand side term in eq 7.45, which is now $(\omega\tau_d/p^2)$, instead of $(\omega\tau_d/p^2)^2$, where τ_d is the longest relaxation time or the reptation time. For the experimental evaluation of this time, besides the instrument accurate temperature control, for minimizing experimental errors, it is required the recording of higher number of data points in the frequency window where the two experimental curves cross. The value measured for the reptation time is also dependent on the constant stress applied to the polymer melt at the viscoelastic linear regime. For this reason, it was ensured the viscoelastic linear regime for unsheared and critically sheared melts and the same stress was used for performing experiments at these two melt states.
(24) Although the saturation of the anisotropy of sheared iPP melts mentioned in Nogales, A.; Olley, R. H.; Mitchell, G. R. *Macromol. Rapid Commun.* **2003**, *24*, 496 refers to melts sheared with a nucleating agent, dibenzylidene sorbitol (DBS), the dimensions of the anisotropic objects evaluated at the saturation by SAXS patterns, ∼500 Å in the flow direction and ∼100 Å in the transverse direction, should indicate the approximate maximum size of precursor structures at the saturation. No saturation was observer for strains lower than 10^3 s.u. Also, it was confirmed experimentally the effect of precursor structures on shear-induced crystallization for much lower strains (see for example ref 12).
(25) In fact, the results obtained do not allow us to conclude definitely whether the recovery of entanglements occurs during the cooling or after the melting. They demonstrate that steady shear experiments performed on critically sheared polymer melts, after a cooling and remelting, are similar to those recorded with unsheared polymer melts. Our assumption that the recovery of entanglements occurs during cooling results from the intimate relationship that exists between entanglements and shear-induced precursor structures, which is demonstrated in this work. Also, since entanglements must result from physical interactions between segments of adjacent chains, partially extended polymer chains coil during the cooling process, thereby increasing the number of interactions between adjacent chain segments. Furthermore, the effect that we are describing must hold both for semicrystalline and amorphous polymer melts.
(26) LeDuc, P.; Haber, C.; Bao, G.; Wirtz, D. *Nature (London)* **1999**, *399*, 564.
(27) Butler, S.; Harrowell, P. *Nature (London)* **2002**, *415*, 1008.
(28) The statement in quotes was made by one reviewer of this work.
(29) Somani, R. H.; Yang, L.; Hsiao, B. *Physica A* **2002**, *304*, 145.
(30) Israelachvili, J. *Intermolecular and Surface Forces*; Academic Press: London, 1992.
(31) Kohler, W. H.; Shrikhande, P.; McHugh, A. J. *J. Macromol. Sci., Part B: Phys.* **2005**, *44*, 185.
(32) Janeschitz-Kriegl, H.; Ratasjski, E.; Stadlbauer, M. *Rheol. Acta* **2003**, *42*, 355.
(33) Janeschitz-Kriegl, H. *Colloid Polym. Sci.* **2003**, *281*, 1157.
(34) Marrucci, G.; Iannirubertо, G. *Macromol. Symp.* **2002**, *185*, 199.
(35) Coppola, S.; Grizzuti, N.; Maffetone, P. L. *Macromolecules* **2001**, *34*, 5030.
(36) Watanabe, H. *Prog. Polym. Sci.* **1999**, *24*, 1253.
(37) Graham, R. S.; Likthman, A. E.; McLeish, T. C. B.; Milner, S. T. *J. Rheol.* **2003**, *47*, 1171.
(38) Marrucci, G. *J. Non-Newtonian Fluid Mech.* **1996**, *62*, 279.
(39) Marrucci, G.; Iannirubertо, G. *J. Non-Newtonian Fluid Mech.* **1996**, *65*, 241.
(40) Likthman, A. E.; Milner, S. T.; McLeish, T. C. B. *Phys. Rev. Lett.* **2000**, *85*, 4550.
(41) McLeish, T. C. B. Present Puzzles of Entangled Polymer Melts. In *Rheology Reviews*; Binding, D. M., Walters, K., Eds.; The British Society of Rheology, 2003; p 197.
(42) Van der Beek, M. H. E.; Peters, G. W. M.; Meijer, H. E. H. *Macromolecules* **2006**, *39*, 1805.
(43) Shanbhag, S.; Larson, R. G. *Macromolecules* **2006**, *39*, 2413.

MA061143U